



# EDGEWOOD CHEMICAL BIOLOGICAL CENTER

U.S. ARMY RESEARCH, DEVELOPMENT AND ENGINEERING COMMAND  
Aberdeen Proving Ground, MD 21010-5424

ECBC-TR-1269

## THERMOPHYSICAL PROPERTIES AND SPECTRAL CHARACTERIZATION OF EA 6043

Patrice L. Abercrombie-Thomas  
Ann Brozena  
James H. Buchanan  
Michael W. Ellzy  
Frederic J. Berg  
Kenneth B. Sumpter  
Phillip G. Wilcox

### RESEARCH AND TECHNOLOGY DIRECTORATE

David E. Tevault

JOINT RESEARCH AND DEVELOPMENT, INC.  
Belcamp, MD 21017-1552

Leonard C. Buettner  
Ian J. Pardoe

EXCET, INC.  
Springfield, VA 22151-2110

Barry R. Williams  
Melissa S. Hulet  
Erik D. Emmons

LEIDOS  
Gunpowder, MD 21010-0068

October 2014

Approved for public release; distribution is unlimited.



#### Disclaimer

The findings in this report are not to be construed as an official Department of the Army position unless so designated by other authorizing documents.

# REPORT DOCUMENTATION PAGE

Form Approved  
OMB No. 0704-0188

Public reporting burden for this collection of information is estimated to average 1 hour per response, including the time for reviewing instructions, searching existing data sources, gathering and maintaining the data needed, and completing and reviewing this collection of information. Send comments regarding this burden estimate or any other aspect of this collection of information, including suggestions for reducing this burden to Department of Defense, Washington Headquarters Services, Directorate for Information Operations and Reports (0704-0188), 1215 Jefferson Davis Highway, Suite 1204, Arlington, VA 22202-4302. Respondents should be aware that notwithstanding any other provision of law, no person shall be subject to any penalty for failing to comply with a collection of information if it does not display a currently valid OMB control number. **PLEASE DO NOT RETURN YOUR FORM TO THE ABOVE ADDRESS.**

<b>1. REPORT DATE (DD-MM-YYYY)</b> XX-10-2014		<b>2. REPORT TYPE</b> Final		<b>3. DATES COVERED (From - To)</b> Jan 1999 – Apr 2014	
<b>4. TITLE AND SUBTITLE</b> Thermophysical Properties and Spectral Characterization of EA 6043				<b>5a. CONTRACT NUMBER</b>	
				<b>5b. GRANT NUMBER</b>	
				<b>5c. PROGRAM ELEMENT NUMBER</b>	
<b>6. AUTHOR(S)</b> Abercrombie-Thomas, Patrice L.; Brozena, Ann; Buchanan, James H.; Ellzy, Michael W.; Berg, Frederic J.; Sumpter, Kenneth B.; Wilcox, Phillip G. (ECBC); Tevault, David E. (JRAD); Buettner, Leonard C.; Pardoe, Ian J. (Excet); Williams, Barry R.; Hulet, Melissa S.; and Emmons, Erik D. (Leidos)				<b>5d. PROJECT NUMBER</b>	
				<b>5e. TASK NUMBER</b>	
				<b>5f. WORK UNIT NUMBER</b>	
<b>7. PERFORMING ORGANIZATION NAME(S) AND ADDRESS(ES)</b> Director, ECBC, ATTN: RDCB-DRC-P, APG, MD 21010-5424 Joint Research and Development, Inc. (JRAD), 4694 Millennium Drive, Suite 105, Belcamp, MD 21017-1552 Excet, Inc., 8001 Braddock Road, Suite 303, Springfield, VA 22151-2110 Leidos, P.O. Box 68, Gunpowder, MD 21010-0068				<b>8. PERFORMING ORGANIZATION REPORT NUMBER</b> ECBC-TR-1269	
<b>9. SPONSORING / MONITORING AGENCY NAME(S) AND ADDRESS(ES)</b> Defense Threat Reduction Agency 8725 John J. Kingman Road, Stop 6201 Fort Belvoir, VA 22060-6201				<b>10. SPONSOR/MONITOR'S ACRONYM(S)</b> DTRA	
				<b>11. SPONSOR/MONITOR'S REPORT NUMBER(S)</b>	
<b>12. DISTRIBUTION/AVAILABILITY STATEMENT</b> Approved for public release; distribution is unlimited.					
<b>13. SUPPLEMENTARY NOTES</b>					
<b>14. ABSTRACT</b> Selected physical and spectroscopic properties of <i>O</i> -( <i>n</i> -butyl)- <i>S</i> -(2-diethylaminoethyl) methylphosphonothiolate, identified in this report as EA 6043, were determined and are reported herein. The title compound is a structural isomer of VX [ <i>O</i> -ethyl- <i>S</i> -(2-diisopropylaminoethyl) methylphosphonothiolate] and Russian VX [ <i>O</i> -isobutyl- <i>S</i> -(2-diethylaminoethyl) methylphosphonothiolate]; and as such, it is also an extremely potent acetylcholinesterase inhibitor. Density, viscosity, surface tension, and vapor pressure for EA 6043 were measured. These properties were correlated to temperature to provide the basis for interpolation and extrapolation of the measured data. Temperature-dependent volatility and heat of vaporization and entropy of vaporization were calculated for EA 6043 on the basis of correlations to the vapor pressure data. Comparisons of selected properties of the structural isomers are provided when possible. Electron impact mass; <sup>1</sup> H, <sup>13</sup> C, and <sup>31</sup> P nuclear magnetic resonance; Fourier transform infrared; and Raman spectra are reported for EA 6043.					
<b>15. SUBJECT TERMS</b>					
EA 6043	VX	Russian VX (RVX)	Density		
Antoine equation	Vapor pressure	Volatility	Enthalpy of vaporization		
Entropy of vaporization	Viscosity	Surface tension	Raman spectrum		
Physical properties	Vapor saturation	Electron impact–mass spectrometry (EI–MS)			
Nuclear magnetic resonance (NMR) spectrum	Fourier transform infrared (FTIR) spectrum				
Differential scanning calorimetry (DSC)	<i>O</i> -( <i>n</i> -butyl)- <i>S</i> -(2-diethylaminoethyl) methylphosphonothiolate				
<b>16. SECURITY CLASSIFICATION OF:</b>			<b>17. LIMITATION OF ABSTRACT</b>	<b>18. NUMBER OF PAGES</b>	<b>19a. NAME OF RESPONSIBLE PERSON</b>
<b>a. REPORT</b>	<b>b. ABSTRACT</b>	<b>c. THIS PAGE</b>			Abercrombie-Thomas, Patrice L
U	U	U	UU	36	<b>19b. TELEPHONE NUMBER (include area code)</b> (410) 436-1740

Blank

## **PREFACE**

The work described in this report was performed between January 1999 and April 2014. This work is documented in laboratory notebook nos. 90-0129, 95-0108, 98-0094, 01-0011, 04-0045, 10-0088, and 10-0041.

The use of either trade or manufacturers' names in this report does not constitute an official endorsement of any commercial products. This report may not be cited for purposes of advertisement.

This report has been approved for public release.

Blank

## CONTENTS

1.	INTRODUCTION.....	1
2.	EXPERIMENTAL METHODS.....	1
3.	RESULTS AND DISCUSSION.....	4
3.1	Density.....	4
3.2	Viscosity.....	6
3.3	Surface Tension.....	8
3.4	Vapor Pressure.....	8
3.5	Electron Impact–Mass Spectrometry.....	14
3.6	Nuclear Magnetic Resonance Spectroscopy.....	15
3.7	FTIR Spectroscopy.....	18
3.8	Raman Spectroscopy.....	19
4.	CONCLUSIONS.....	21
	LITERATURE CITED.....	23
	ACRONYMS AND ABBREVIATIONS.....	25

## FIGURES

1. Molecular structure of EA 6043 .....	1
2. Liquid density and linear correlation for EA 6043 .....	5
3. Liquid density for EA 6043 relative to VX, RVX, seawater, and fresh water .....	5
4. Viscosity of EA 6043 and Antoine correlation .....	7
5. Viscosity of EA 6043 relative to VX and RVX .....	7
6. Surface tension of EA 6043 relative to VX and RVX .....	8
7. Vapor pressure and Antoine correlation for EA 6043 .....	12
8. Vapor pressure comparison of EA 6043, VX, and RVX .....	13
9. EI-MS of EA 6043 .....	14
10. <sup>1</sup> H NMR spectrum of EA 6043 .....	15
11. <sup>13</sup> C NMR spectrum of EA 6043 .....	16
12. <sup>31</sup> P NMR spectrum of EA 6043 .....	17
13. FTIR spectrum at 400–4000 cm <sup>-1</sup> for liquid-phase EA 6043 .....	18
14. FTIR spectrum at 600–4000 cm <sup>-1</sup> for vapor-phase EA 6043 .....	18
15. Raman spectrum of liquid-phase EA 6043 at $\Delta\nu = 400\text{--}3600\text{ cm}^{-1}$ .....	19

## TABLES

1. Sample Identification .....	2
2. Experimental and Correlated Density of EA 6043 .....	4
3. Experimental and Correlated Viscosity of EA 6043 .....	6
4. Surface Tension of EA 6043 .....	8
5. Experimental and Calculated Vapor Pressure and Percent Differences for EA 6043 .....	9
6. Antoine Equation Vapor Pressure Coefficients for EA 6043 .....	10
7. Calculated Properties of EA 6043 at Selected Temperatures .....	11
8. Physical Properties of EA 6043, VX, and RVX .....	14
9. FTIR Absorption and Raman Shift Frequencies for EA 6043 .....	20

# THERMOPHYSICAL PROPERTIES AND SPECTRAL CHARACTERIZATION OF EA 6043

## 1. INTRODUCTION

Selected physical and spectral properties of toxic chemical warfare agents and their surrogates and precursors have been measured and reported<sup>1-8</sup> in our laboratory using a variety of intact and modified methods established by ASTM International (West Conshohocken, PA). This report documents selected physical properties and spectral characteristics of *O*-(*n*-butyl)-*S*-(2-diethylaminoethyl) methylphosphonothiolate, which is a highly toxic nerve agent identified in this report as EA 6043. The molecular structure of EA 6043 is shown in Figure 1.

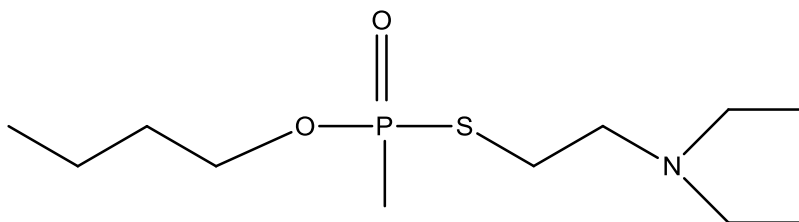


Figure 1. Molecular structure of EA 6043.

The physical properties for EA 6043 reported herein include density, viscosity, surface tension, and vapor pressure. When possible, these results were correlated with temperature, which provides the basis for interpolation and extrapolation of the measured data. Spectral data, including electron impact–mass spectrometry (EI–MS); proton (<sup>1</sup>H), carbon-13 (<sup>13</sup>C), and phosphorus-31 (<sup>31</sup>P) nuclear magnetic resonance (NMR); and Fourier transform infrared (FTIR) and Raman spectroscopy, were measured and are also provided in this report. Previous reports include similar data for two isomers of EA 6043: VX [*O*-ethyl-*S*-(2-diisopropylaminoethyl) methylphosphonothiolate] and Russian VX (RVX) [*O*-isobutyl-*S*-(2-diethylaminoethyl) methylphosphonothiolate].<sup>5-7</sup>

## 2. EXPERIMENTAL METHODS

EA 6043, as its better-known isomers VX and RVX, is a potent cholinesterase inhibitor and should only be handled by highly skilled workers in specially designed facilities under strict engineering controls. The samples used in the current work were synthesized, purified, and analyzed for purity in house.

This work was performed using samples of varying purity. Sample lot number and purity information are provided in Table 1. In 1999, the density, viscosity, and surface tension of EA 6043 were determined at 20 and 35 °C using a 92% pure sample, and the vapor pressure was measured using vapor saturation on a 94% pure sample. In 2003, the density and viscosity of EA 6043 were determined at 25, 35, and 50 °C, and the surface tension was determined at 25 °C using a 94% pure sample. In 2004, the vapor pressure of EA 6043 was determined using differential scanning calorimetry (DSC) with a 94.5% pure sample. In 2014, the spectral data for EA 6043 were measured using a 94.9% pure sample.

Table 1. Sample Identification

Year	Sample Number	Property	Purity (mole fraction)
1999	98-0094-12.1	Density (20 and 35 °C) Viscosity (20 and 35 °C) Surface tension (20 and 35 °C)	0.920
1999	98-0094-13.1	Vapor pressure, saturator	0.940
2003	99-0003-128	Density (25, 35, and 50 °C) Viscosity (25, 35, and 50 °C) Surface tension (25 °C)	0.940
2004	98-0094-144.2	Vapor pressure, DSC	0.945
2014	98-0094-144.2	NMR spectra Liquid-phase FTIR spectrum Vapor-phase FTIR spectrum Raman spectrum EI-MS	0.949

Liquid density was determined as a function of temperature in accordance with ASTM D 4052, *Standard Test Method for Density, Relative Density, and API Gravity of Liquids by Digital Density Meter*<sup>9</sup> using an Anton Paar (Anton Paar USA Inc., Ashland, VA) model DMA 58 digital density meter. This measurement is based on the change in frequency of an oscillating U-tube due to the presence of the test specimen. Before sample measurements, the instrument was calibrated at the experimental temperatures using air and distilled water. Proper instrument operation was validated using toluene, a National Institute of Standards and Technology (NIST) standard.

Viscosity was determined as a function of temperature in accordance with ASTM D 445, *Standard Test Method for Kinematic Viscosity of Transparent and Opaque Liquids (the Calculation of Dynamic Viscosity)*<sup>10</sup> using a Cannon-Manning semi-micro viscometer and Cannon CT-1000 constant temperature bath (Cannon Instrument Company; State College, PA). In this method, viscosity is determined by measuring the flow rate of a liquid through a calibrated glass capillary viscometer. The viscometer used for this work was calibrated by the manufacturer.

Surface tension measurements were performed using a KRÜSS (Hamburg, Germany) K12 tensiometer with an external Lauda (Lauda-Brinkman, LP; Delran, NJ) RM-6 circulating bath, in accordance with *Determination of the Surface Tension of Liquids Using the Wilhelmy Plate Method*, which is located in the appendix of ECBC-TR-804.<sup>11</sup> This method is used to determine the force per unit length required to overcome intermolecular forces at the liquid-air interface. For this work, a small rectangular glass plate is vertically suspended over the liquid with the bottom edge parallel to the surface. The liquid is then raised until it just touches the bottom edge of the plate. The force on the plate increases due to wetting of the liquid against the plate. Surface tension is determined at the point where the contact angle between the liquid and the plate is zero due to perfect wetting.<sup>12</sup> Proper operation of the tensiometer was validated using a diethyl oxalate standard.

The vapor pressure of EA 6043 was determined using two modified ASTM methods, DSC at high temperatures (140.7 to 240.2 °C) and gas saturation in the ambient temperature range (-15.1 to 6.0 °C). DSC vapor pressure measurements were performed in accordance with ASTM E 1782, *Standard Test Method for Determining Vapor Pressure by Thermal Analysis*.<sup>13</sup> A TA Instruments (New Castle, DE) 910 DSC and 2200 controller were used in the present work. Before sample measurements were performed, the DSC was calibrated using indium and water in accordance with ASTM E 967, *Standard Test Method for Temperature Calibration of Differential Scanning Calorimeters and Differential Thermal Analyzers*.<sup>14</sup>

A modified version of ASTM E 1194, *Standard Test Method for Vapor Pressure*<sup>15</sup> was used in this work. Vapor saturation measurements were performed using the apparatus described previously, including a Hewlett-Packard (Palo Alto, CA) model 5890 series II gas chromatograph (GC) equipped with a flame photometric detector with a phosphorus filter (FPD-P).<sup>6</sup> The glass saturator used in this effort was custom-designed in our laboratory.

The equipment and procedures used to generate saturated streams in the present work are identical to those used previously to measure ambient temperature vapor pressure data in our laboratory and are summarized herein. A saturated vapor stream was generated using the saturator cell at a known temperature. Nitrogen carrier gas was introduced at a controlled mass flow rate over a known time, the analyte was collected using the Dynatherm sample concentrator (Dynatherm Analytical Instruments, Inc. from CDS Analytical, Inc.; Oxford, PA), and the mass was quantified using GC-FPD analysis.

Saturated vapor streams were generated by flowing dry nitrogen carrier gas at 30.0 sccm through the saturator cell that contained liquid EA 6043. The EA 6043 was analyzed using NMR before and after vapor pressure data were measured. Vapor pressures were calculated as in the VX and RVX reports.<sup>5-7</sup>

All NMR spectra for EA 6043 were recorded in CDCl<sub>3</sub> on a JEOL (JEOL USA, Inc.; Peabody, MA) ECX-400 NMR instrument. The <sup>1</sup>H and <sup>13</sup>C spectra were referenced to the solvent signal. The <sup>31</sup>P NMR was referenced to H<sub>3</sub>PO<sub>4</sub>.

The mass spectrum was recorded using a Hewlett-Packard 5975 series mass selective detector coupled to a Hewlett-Packard 6890 GC.

The FTIR spectrum of EA 6043 was collected as a 10 μm film between KBr plates on a Nicolet 680 FTIR system using a triglycine sulfate (TGS) detector. The vapor-phase FTIR spectrum was measured using a Nicolet (Thermo Scientific Dionex; Sunnyvale, CA) 6700 FTIR system equipped with a mercury-cadmium telluride (MCT) detector that was interfaced to a GC with a light-pipe accessory. FTIR spectra were recorded at 4 cm<sup>-1</sup> resolution.

The Raman spectrum of EA 6043 was measured as neat material using a near-infrared NIR 700 Raman spectrometer from EIC Laboratories, Inc. (Norwood, MA) that was equipped with an InPhotonics (InPhotonics, Inc.; Norwood, MA) RamanProbe and a 3 m fiber-optic cable. The Raman instrument included an SDL model 8530 diode laser operating at 785 nm and an Andor iDus 420-OE charge-coupled device (CCD) camera. The laser power at the sample was approximately 150 mW. The spectral resolution was approximately 1 cm<sup>-1</sup>.

### 3. RESULTS AND DISCUSSION

#### 3.1 Density

The experimental density data for EA 6043 for the 1999 and 2003 samples are provided in Table 2. These data and the calculated linear fit for the higher purity 2003 sample are plotted in Figure 2. In the ambient temperature range, the density of EA 6043 is approximately 0.4% higher than that of VX and 0.6% higher than that of RVX.<sup>5</sup>

Table 2. Experimental and Correlated Density of EA 6043

Year	Temperature (°C)	Density* (g/mL)		Percent Difference**
		Experimental	Calculated	
1999	20.0	1.01172	N/A	N/A
	35.0	0.99940	N/A	N/A
2003	25.0	1.01255	1.01253	0.002
	35.0	1.00409	1.00412	-0.003
	50.0	0.99150	0.99149	0.001

N/A: not applicable

\*The uncertainty of each measurement is  $\leq 0.00005$  g/mL

\*\*Percent difference is calculated using  $[(\text{experimental} - \text{calculated})/\text{calculated}] \times 100$

The correlation between density ( $\rho$ ) and temperature at 25–50 °C for EA 6043 is given by eq 1,

$$\rho = a + b \times t \quad (1)$$

where

$$\begin{aligned} \rho &= \text{density (g/mL)} \\ t &= \text{temperature (°C)} \\ a &= 1.03358 \\ b &= -8.42 \times 10^{-4} \end{aligned}$$

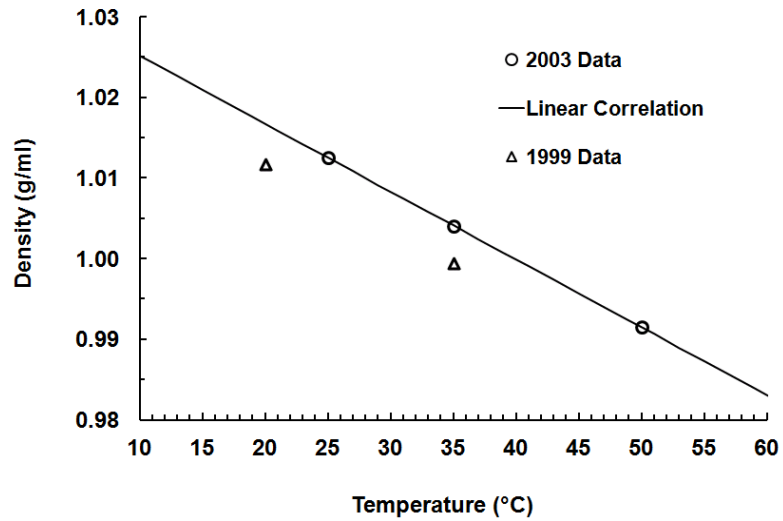


Figure 2. Liquid density and linear correlation for EA 6043.

The 1999 density data, shown as triangles in Figure 2, clearly demonstrate that the measured density of EA 6043 depends on sample purity. As shown in Figure 3, EA 6043 is denser than fresh water<sup>16</sup> at ambient temperatures, but it is less dense than seawater (35 g of solids/L) at all practical temperatures above approximately 8 °C.<sup>17</sup> Similarly, VX and RVX are denser than fresh water and less dense than seawater at virtually all practical temperatures.

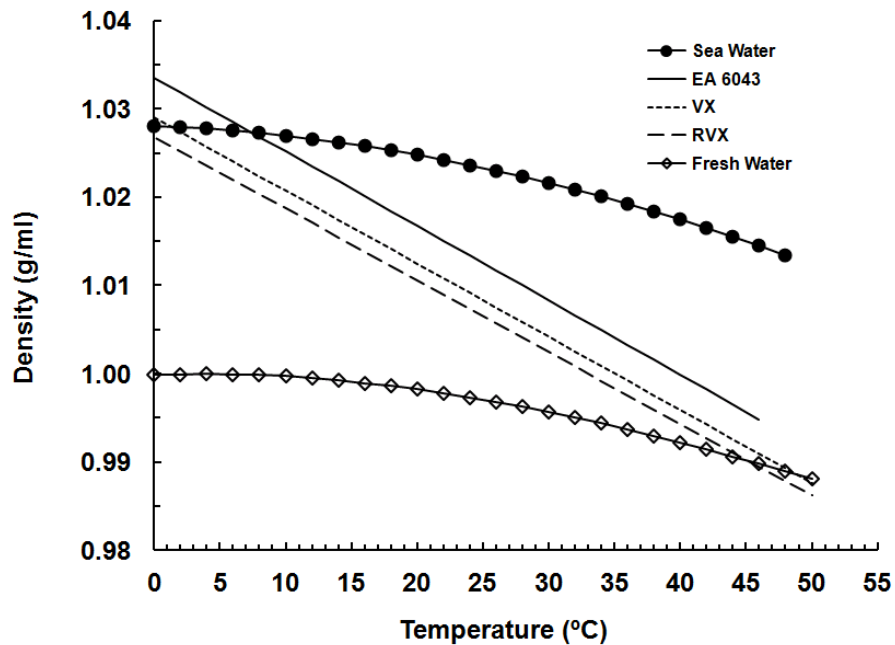


Figure 3. Liquid density for EA 6043 relative to VX, RVX, seawater, and fresh water.

### 3.2 Viscosity

The experimental kinematic viscosity data for EA 6043 are listed in Table 3.

Table 3. Experimental and Correlated Viscosity of EA 6043

Year	Temperature (°C)	Viscosity (cSt)		Percent Difference**
		Experimental*	Calculated	
1999	20.0	9.27 (0.02)	N/A	N/A
	35.0	5.65 (0.01)	N/A	N/A
2003	25.0	9.29 (0.02)	9.290	0.00
	35.0	6.48 (0.01)	6.484	-0.06
	50.0	4.02 (0.01)	4.017	0.07

N/A: not applicable

\*Standard deviation (in parentheses) is  $\leq 0.02$  cSt

\*\*Percent difference is calculated:  $[(\text{experimental} - \text{calculated})/\text{calculated}] \times 100$

The correlation between the higher purity (2003) viscosity data and temperature at 25 to 50 °C is given (eq 2) by the Antoine equation,<sup>18</sup>

$$\log(\eta) = A - B/(C + t) \quad (2)$$

where

$$\begin{aligned} \eta &= \text{viscosity (centistokes, cSt)} \\ t &= \text{temperature (°C)} \\ A &= -2.27468 \\ B &= -640.840 \\ C &= 172.627 \end{aligned}$$

The viscosity data and Antoine correlation for EA 6043 are plotted in Figure 4. Figure 5 illustrates a comparison of the viscosity of EA 6043 to that of VX and RVX; the viscosity of EA 6043 at 25 °C is approximately 2% higher than RVX and about 7% lower than VX.

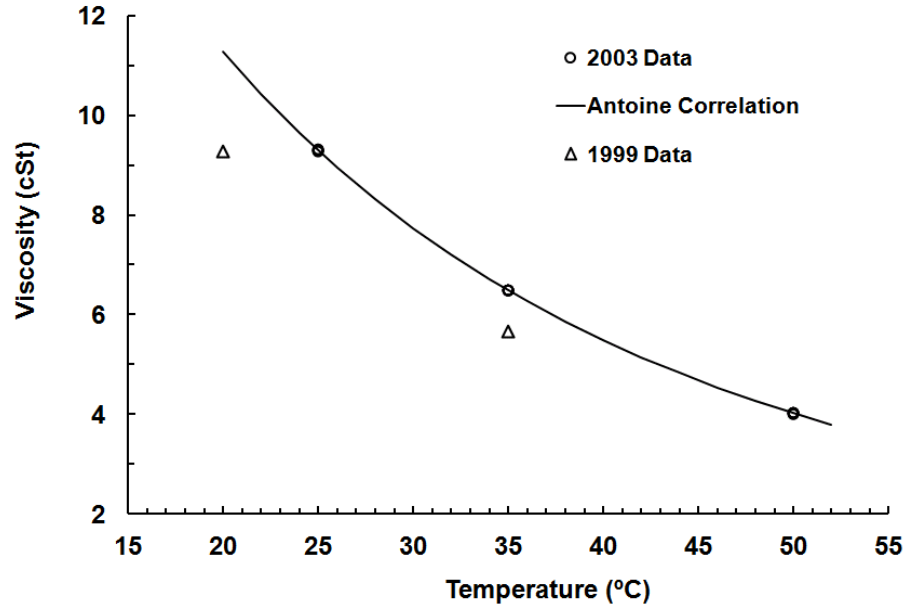


Figure 4. Viscosity of EA 6043 and Antoine correlation.

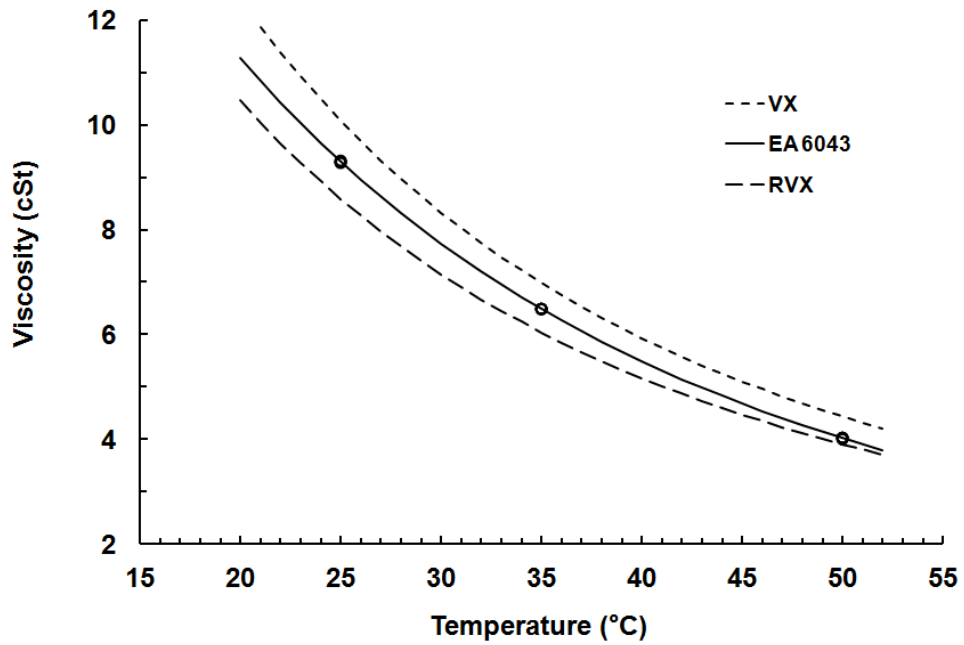


Figure 5. Viscosity of EA 6043 relative to VX and RVX.

### 3.3 Surface Tension

Surface tension data for EA 6043 are listed in Table 4 and plotted in Figure 6 with correlations for VX and RVX.<sup>5</sup> Each experimental value reported for EA 6043 is the mean of 10 measurements for each specimen. The surface tension of EA 6043 is lower than VX by 25% and RVX by 16%.

Table 4. Surface Tension of EA 6043

Year	Temperature (°C)	Surface Tension (dyn/cm)	Standard Deviation
1999	20.0	22.3	0.2
	35.0	21.0	0.3
2003	25.0	22.68	0.03

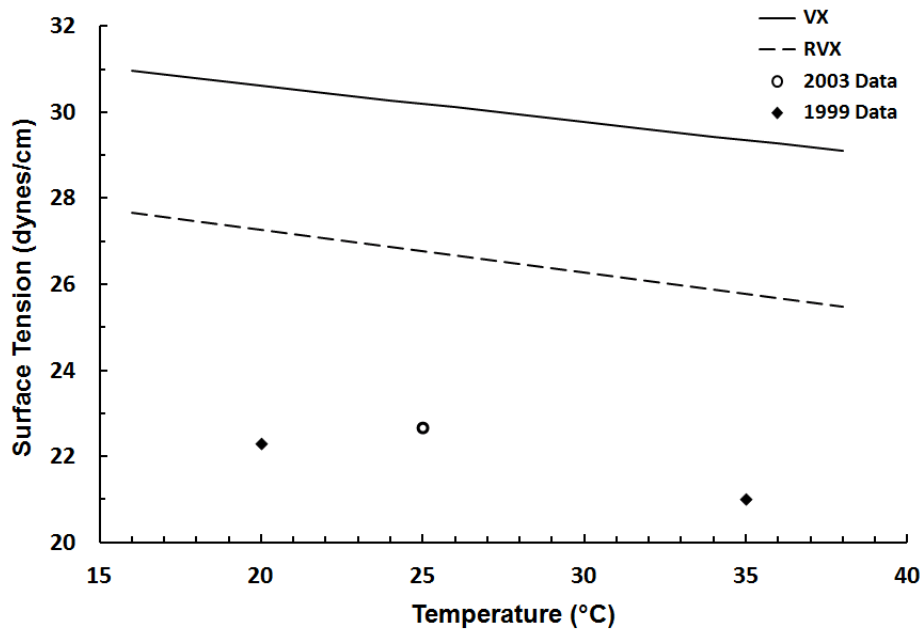


Figure 6. Surface tension of EA 6043 relative to VX and RVX.

### 3.4 Vapor Pressure

Vapor pressure measurements were obtained for EA 6043 between  $-15.1$  and  $6.0$  °C using the gas saturation method and between  $140.7$  and  $240.2$  °C using the DSC method. These measurements span a pressure range of more than 8 orders of magnitude. The experimental vapor pressure data obtained using these two complementary techniques are listed in Table 5.

Table 5. Experimental and Calculated Vapor Pressure and Percent Differences for EA 6043

Temperature		P <sub>exp</sub>		P <sub>calc</sub>		Percent Difference*
°C	K	torr	Pa	torr	Pa	
Vapor Saturation						
-15.1	258.05	6.03 × 10 <sup>-7</sup>	8.04 × 10 <sup>-5</sup>	6.313 × 10 <sup>-7</sup>	8.417 × 10 <sup>-5</sup>	-4.48
-10.0	263.15	1.45 × 10 <sup>-6</sup>	1.93 × 10 <sup>-4</sup>	1.559 × 10 <sup>-6</sup>	2.078 × 10 <sup>-4</sup>	-7.14
-5.0	268.15	2.94 × 10 <sup>-6</sup>	3.92 × 10 <sup>-4</sup>	3.606 × 10 <sup>-6</sup>	4.808 × 10 <sup>-4</sup>	-18.47
0.0	273.15	1.01 × 10 <sup>-5</sup>	1.35 × 10 <sup>-3</sup>	7.989 × 10 <sup>-6</sup>	1.065 × 10 <sup>-3</sup>	26.74
1.0	274.15	1.09 × 10 <sup>-5</sup>	1.45 × 10 <sup>-3</sup>	9.321 × 10 <sup>-6</sup>	1.243 × 10 <sup>-3</sup>	16.68
6.0	279.15	1.95 × 10 <sup>-5</sup>	2.60 × 10 <sup>-3</sup>	1.969 × 10 <sup>-5</sup>	2.625 × 10 <sup>-3</sup>	-0.93
DSC						
140.67	413.82	2.4	3.20 × 10 <sup>2</sup>	2.422	3.229 × 10 <sup>2</sup>	-0.90
159.99	433.14	5.8	7.70 × 10 <sup>2</sup>	6.255	8.340 × 10 <sup>2</sup>	-7.28
173.06	446.21	10.3	1.370 × 10 <sup>3</sup>	11.23	1.497 × 10 <sup>3</sup>	-8.28
188.07	461.22	20.4	2.720 × 10 <sup>3</sup>	20.93	2.791 × 10 <sup>3</sup>	-2.54
203.24	476.39	36.7	4.890 × 10 <sup>3</sup>	37.43	4.991 × 10 <sup>3</sup>	-1.96
211.18	484.33	50.4	6.720 × 10 <sup>3</sup>	49.88	6.650 × 10 <sup>3</sup>	1.05
223.29	496.44	78.5	1.047 × 10 <sup>4</sup>	75.65	1.009 × 10 <sup>4</sup>	3.77
233.15	506.30	101.4	1.352 × 10 <sup>4</sup>	104.4	1.391 × 10 <sup>4</sup>	-2.83
240.23	513.38	150.8	2.011 × 10 <sup>4</sup>	130.3	1.737 × 10 <sup>4</sup>	15.75

P<sub>exp</sub>: experimental vapor pressure

P<sub>calc</sub>: calculated vapor pressure

\*Percent difference is calculated: [(experimental – calculated)/calculated] × 100

This combined data set was fitted to a three-parameter Antoine equation by minimizing the sum of the squares of the log-differences between the measured and calculated values. The Antoine constants with the corresponding Antoine equations are listed in Table 6 using two common pressure unit systems: temperature in kelvin with pressure in pascal and temperature in Celsius with pressure in torr.

The percent differences between the measured and calculated values provide an indication of the accuracy and precision of this data set over the experimental range. We have observed closer agreement between experimental and calculated values for more volatile materials.

Table 6. Antoine Equation Vapor Pressure Coefficients for EA 6043

$\ln(P_{Pa}) = a - b/(c + T_K)$		
<i>a</i>	<i>b</i>	<i>c</i>
23.13829	5801.300	-79.66333
Temperature ( <i>T</i> ) range: 258.0 to 513.4 K		
$\log(P_{torr}) = A - B/(C + t_C)$		
<i>A</i>	<i>B</i>	<i>C</i>
7.923927	2519.473	193.4867
Temperature ( <i>t</i> ) range: -15.1 to 240.2 °C		

Equations 3 and 4 were used to calculate the heat of vaporization (kJ/mol) and volatility (mg/m<sup>3</sup>), respectively, as a function of temperature.

$$\Delta H_{\text{vap}} = RbT^2/(c + T)^2 \quad (3)$$

where

$$\begin{aligned} \Delta H_{\text{vap}} &= \text{enthalpy of vaporization (kJ/mol)} \\ R &= \text{gas constant [8.3144 J/(K mol)]} \\ b, c &= \text{Antoine constants} \\ T &= \text{temperature (K)} \end{aligned}$$

and

$$V = PM/RT \quad (4)$$

where

$$\begin{aligned} V &= \text{volatility (mg/m}^3\text{)} \\ P &= \text{vapor pressure (Pa)} \\ M &= \text{molecular weight (g/mol)} \end{aligned}$$

Table 7 shows the calculated values using the Antoine coefficients (Table 6) for vapor pressure, volatility (or saturation concentration), and enthalpy of vaporization at selected temperatures between -20 °C and the calculated normal boiling point.

Table 7. Calculated Properties of EA 6043 at Selected Temperatures

Temperature (°C)	Vapor Pressure		Volatility (mg/m <sup>3</sup> )	$\Delta H_{\text{vap}}$	
	torr	Pa		(kcal/mol)	(kJ/mol)
-20*	$2.520 \times 10^{-7}$	$3.359 \times 10^{-5}$	$4.267 \times 10^{-3}$	24.55	102.70
-10	$1.559 \times 10^{-6}$	$2.078 \times 10^{-4}$	$2.539 \times 10^{-2}$	23.71	99.21
0	$7.989 \times 10^{-6}$	$1.065 \times 10^{-3}$	$1.254 \times 10^{-1}$	22.98	96.13
10	$3.487 \times 10^{-5}$	$4.649 \times 10^{-3}$	$5.278 \times 10^{-1}$	22.32	93.39
20	$1.326 \times 10^{-4}$	$1.767 \times 10^{-2}$	$1.938 \times 10^0$	21.74	90.95
25	$2.469 \times 10^{-4}$	$3.291 \times 10^{-2}$	$3.550 \times 10^0$	21.47	89.82
30	$4.471 \times 10^{-4}$	$5.961 \times 10^{-2}$	$6.323 \times 10^0$	21.21	88.75
40	$1.359 \times 10^{-3}$	$1.812 \times 10^{-1}$	$1.861 \times 10^1$	20.74	86.76
50	$3.771 \times 10^{-3}$	$5.028 \times 10^{-1}$	$5.003 \times 10^1$	20.31	84.96
60	$9.653 \times 10^{-3}$	$1.287 \times 10^0$	$1.242 \times 10^2$	19.91	83.32
70	$2.301 \times 10^{-2}$	$3.067 \times 10^0$	$2.874 \times 10^2$	19.55	81.81
80	$5.146 \times 10^{-2}$	$6.861 \times 10^0$	$6.247 \times 10^2$	19.22	80.43
100	$2.184 \times 10^{-1}$	$2.912 \times 10^1$	$2.509 \times 10^3$	18.64	77.97
120	$7.709 \times 10^{-1}$	$1.028 \times 10^2$	$8.408 \times 10^3$	18.13	75.86
140	$2.339 \times 10^0$	$3.118 \times 10^2$	$2.427 \times 10^4$	17.69	74.03
160	$6.258 \times 10^0$	$8.343 \times 10^2$	$6.194 \times 10^4$	17.31	72.42
180	$1.507 \times 10^1$	$2.009 \times 10^3$	$1.426 \times 10^5$	16.97	71.01
200	$3.319 \times 10^1$	$4.425 \times 10^3$	$3.007 \times 10^5$	16.67	69.74
220	$6.772 \times 10^1$	$9.028 \times 10^3$	$5.887 \times 10^5$	16.40	68.61
240	$1.294 \times 10^2$	$1.725 \times 10^4$	$1.081 \times 10^6$	16.15	67.59
260*	$2.334 \times 10^2$	$3.112 \times 10^4$	$1.877 \times 10^6$	15.93	66.67
280*	$4.007 \times 10^2$	$5.342 \times 10^4$	$3.106 \times 10^6$	15.73	65.83
300*	$6.584 \times 10^2$	$8.778 \times 10^4$	$4.925 \times 10^6$	15.55	65.06
306.10*	$7.600 \times 10^2$	$1.01325 \times 10^5$	$5.625 \times 10^6$	15.50	64.84

\*Extrapolated

As observed for VX and RVX, the data measurement for EA 6043 presented a problem for the gas saturation method; this was due, in part, to interactions with the vapor-transfer lines. Measures to minimize these effects (e.g., use of heated transfer lines, specially coated tubing, and extended data collection time to facilitate achievement of a steady state), have improved the reproducibility of the data. However, it should be noted that the differences between the experimental data and correlated values for this compound were as high as 27%. The data reported for the gas saturation method represent averages of at least 10 measurements each.

The agreement between the vapor pressure data measured using the two methods enhances confidence that both methods produced accurate data. The temperature gap between the data sets (135 °C) is unusually large, and steps were taken recently to modify both methods to close the gap. Since completion of the present work, the DSC method has been modified to produce accurate data as low as 200 Pa for *n*-octanol<sup>19</sup> through the use of larger pinholes than prescribed for that method. As a result of that work, the ASTM procedure for measuring vapor pressure using thermal methods was modified to extend the low-pressure limit from 5000 to 200 Pa. In addition, heat-tracing the sample-transfer line back to the ethylene glycol water bath using submersible heat tape increased the dynamic range of the saturator method to above 50 °C.

A plot of the experimental DSC and saturator data and the calculated Antoine correlation is shown in Figure 7. The normal boiling temperature calculated for EA 6043 based on this data is 306.10 °C. A comparison of EA 6043 vapor pressure correlations with those of VX and RVX is shown in Figure 8.

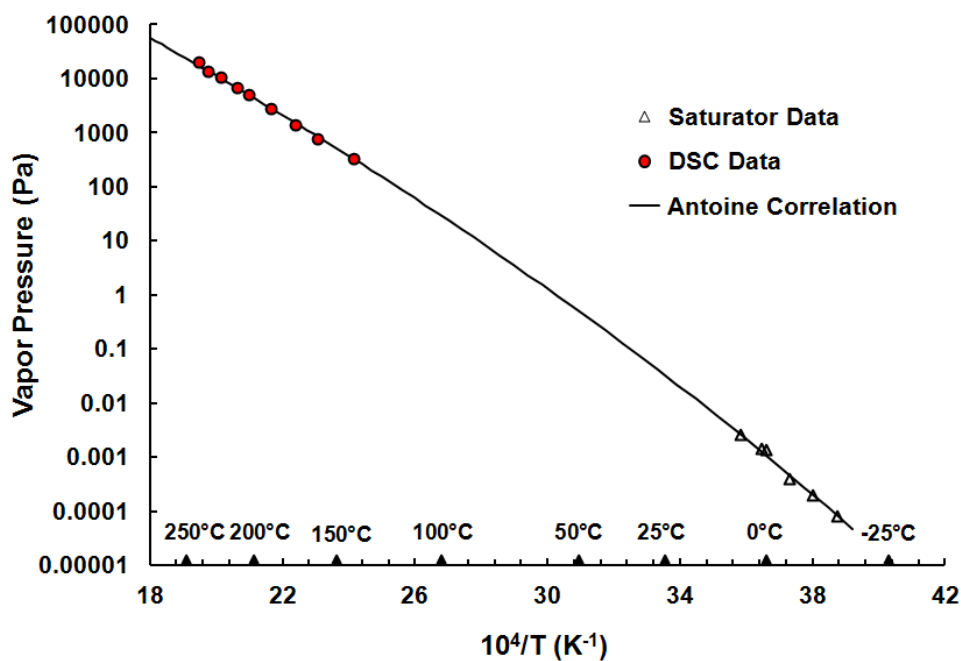


Figure 7. Vapor pressure and Antoine correlation for EA 6043.

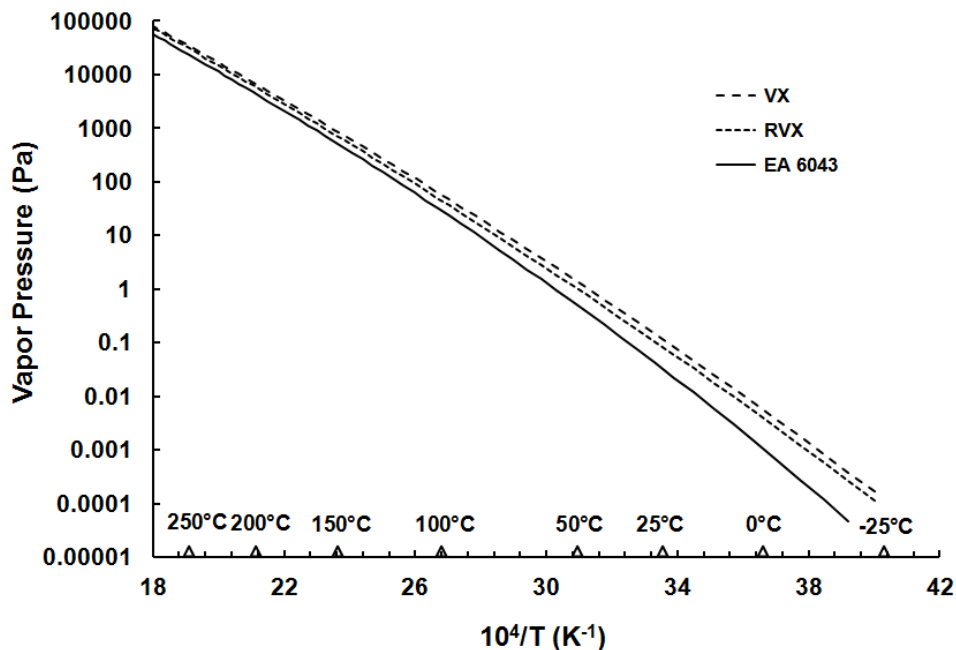


Figure 8. Vapor pressure comparison of EA 6043, VX, and RVX.

The entropy of vaporization for EA 6043, calculated based on the current analysis, is 111.9 J/mol-K, which is higher than the value of 87 J/mol-K suggested by Trouton's rule. The entropy of vaporization values for VX and RVX are 113.5 and 116.2 J/mol-K, respectively. The reason for this variation among the three isomers, when compared with the value predicted by Trouton's rule, is unknown at this time.

Selected physical properties of EA 6043, VX, and RVX at 25 °C, based on the data correlations developed in this work, are summarized in Table 8.

Table 8. Physical Properties of EA 6043, VX, and RVX

Property	EA 6043	VX	RVX
Vapor pressure at 25 °C (Pa)	$3.291 \times 10^{-2}$	$1.17 \times 10^{-1}$	$8.40 \times 10^{-2}$
Vapor pressure at 25 °C (torr)	$2.469 \times 10^{-4}$	$8.78 \times 10^{-4}$	$6.30 \times 10^{-4}$
Volatility at 25 °C (mg/m <sup>3</sup> )	3.550	12.6	9.06
Normal boiling point (°C)	306.1	291.6	294.7
Density at 25 °C (g/mL)	1.0125	1.0083	1.0064
Viscosity at 25 °C (cSt)	9.29	10.09	8.58
Surface tension at 25 °C (dynes/cm)	22.68	30.20	26.89
Entropy of vaporization (J/mol-K)	111.9	113.5	116.2

### 3.5 Electron Impact–Mass Spectrometry

The EI–MS of EA 6043 (Figure 9), was recorded using a Hewlett-Packard 5975 series mass selective detector coupled to a Hewlett-Packard 6890 GC. The resulting mass-to-charge ratio ( $m/z$ ) values, with relative intensities shown in parentheses, are 44 (3), 56 (4), 57 (4), 58 (4), 71 (8), 86 (100), 99 (33), 100 (5), 139 (3), 195 (1). A small feature near 267  $m/z$  is probably associated with the parent ion.

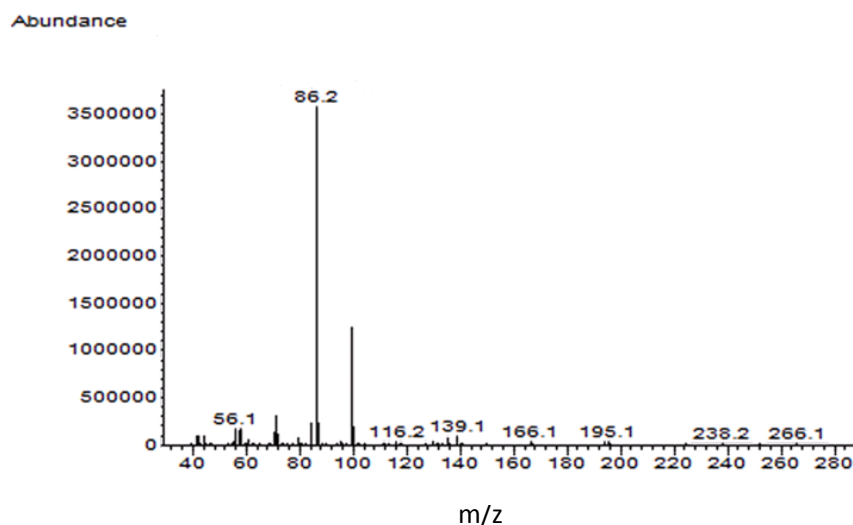


Figure 9. EI-MS of EA 6043.

### 3.6 Nuclear Magnetic Resonance Spectroscopy

$^1\text{H}$ ,  $^{13}\text{C}$ , and  $^{31}\text{P}$  NMR spectra were obtained for EA 6043 and are illustrated in Figures 10–12, respectively. Details of the NMR spectra follow:

$^1\text{H}$  NMR ( $\text{CDCl}_3$ ,  $\delta$ ): 3.86 (multiple peaks,  $\text{OCH}_2\text{CH}_2\text{CH}_2\text{CH}_3$ ), 2.73 (multiple peaks,  $\text{SCH}_2\text{CH}_2\text{N}$ ), 2.53 (multiple peaks,  $\text{SCH}_2\text{CH}_2\text{N}$ ), 2.37 (quartet,  $J = 6.9$  Hz  $\text{NCH}_2\text{CH}_3$ ), 1.59 (doublet of doublets,  $J = 15.6, 1$  Hz,  $\text{P-CH}_3$ ), 1.46 (quintuplet,  $J = 6.9$  Hz,  $\text{OCH}_2\text{CH}_2\text{CH}_2\text{CH}_3$ ), 1.20 (sextet,  $J = 7.3$  Hz,  $\text{OCH}_2\text{CH}_2\text{CH}_2\text{CH}_3$ ), 0.84 (triplet,  $J = 6.4$  Hz  $\text{NCH}_2\text{CH}_3$ ), 0.74 (triplet,  $J = 7.2$  Hz,  $\text{OCH}_2\text{CH}_2\text{CH}_2\text{CH}_3$ ).

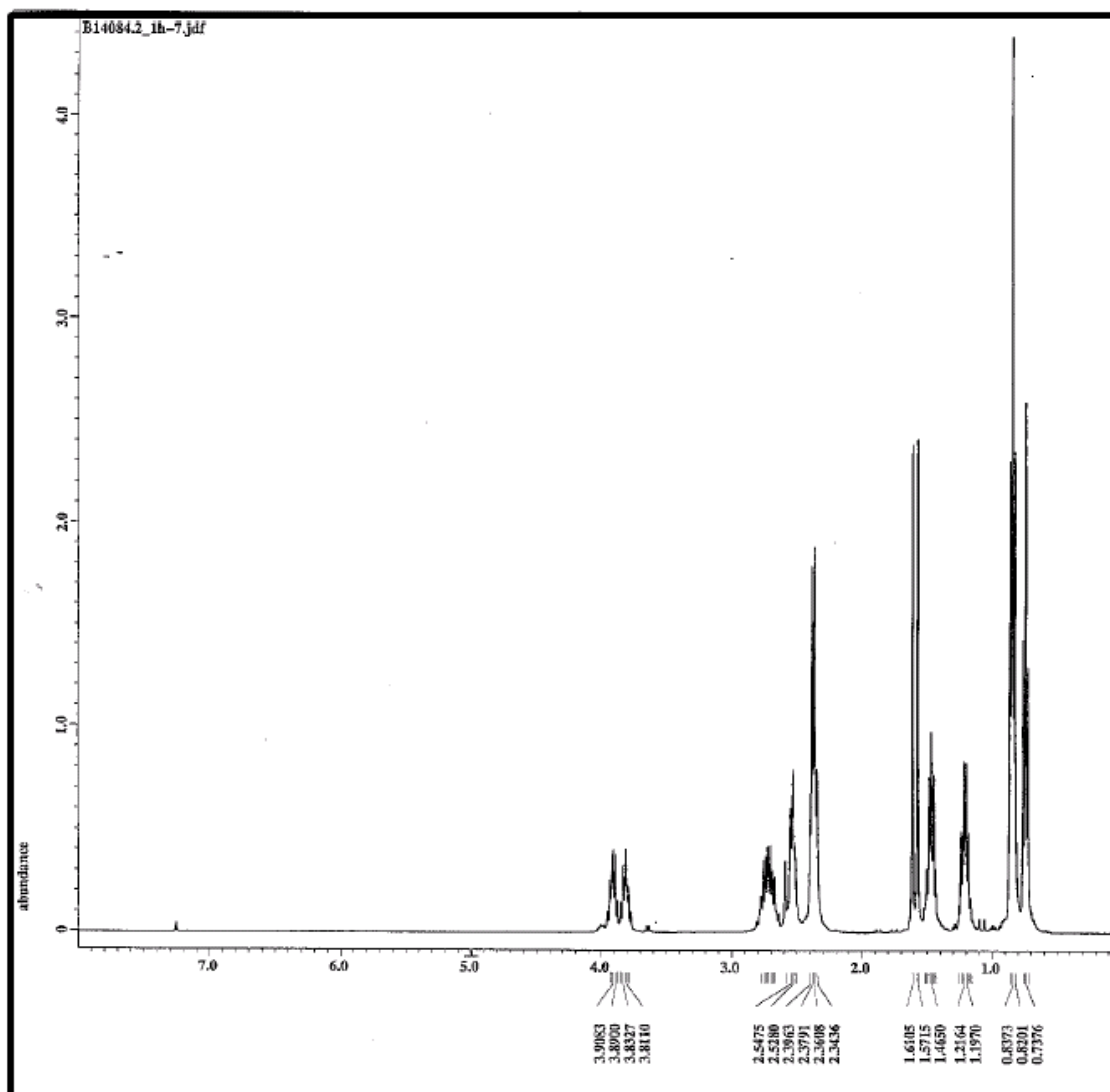


Figure 10.  $^1\text{H}$  NMR spectrum of EA 6043.

$^{13}\text{C}$  NMR ( $\text{CDCl}_3$ ,  $\delta$ ): 64.7 (doublet,  $J = 6.7$  Hz,  $\text{OCH}_2\text{CH}_2\text{CH}_2\text{CH}_3$ ), 53.6 (doublet,  $J = 3.8$  Hz,  $\text{SCH}_2\text{CH}_2\text{N}$ ), 46.9 (singlet,  $\text{NCH}_2\text{CH}_3$ ), 32.2 (doublet,  $J = 6.7$  Hz,  $\text{OCH}_2\text{CH}_2\text{CH}_2\text{CH}_3$ ), 28.1 (singlet,  $\text{SCH}_2\text{CH}_2\text{N}$ ), 20.0 (doublet,  $J = 110$  Hz,  $\text{P-CH}_3$ ), 18.7 (doublet,  $J = 11.5$  Hz,  $\text{OCH}_2\text{CH}_2\text{CH}_2\text{CH}_3$ ), 13.5 (singlet,  $\text{OCH}_2\text{CH}_2\text{CH}_2\text{CH}_3$ ), 11.8 (singlet,  $\text{NCH}_2\text{CH}_3$ ). The triplet centered at about 77.35 ppm is characteristic of the solvent.

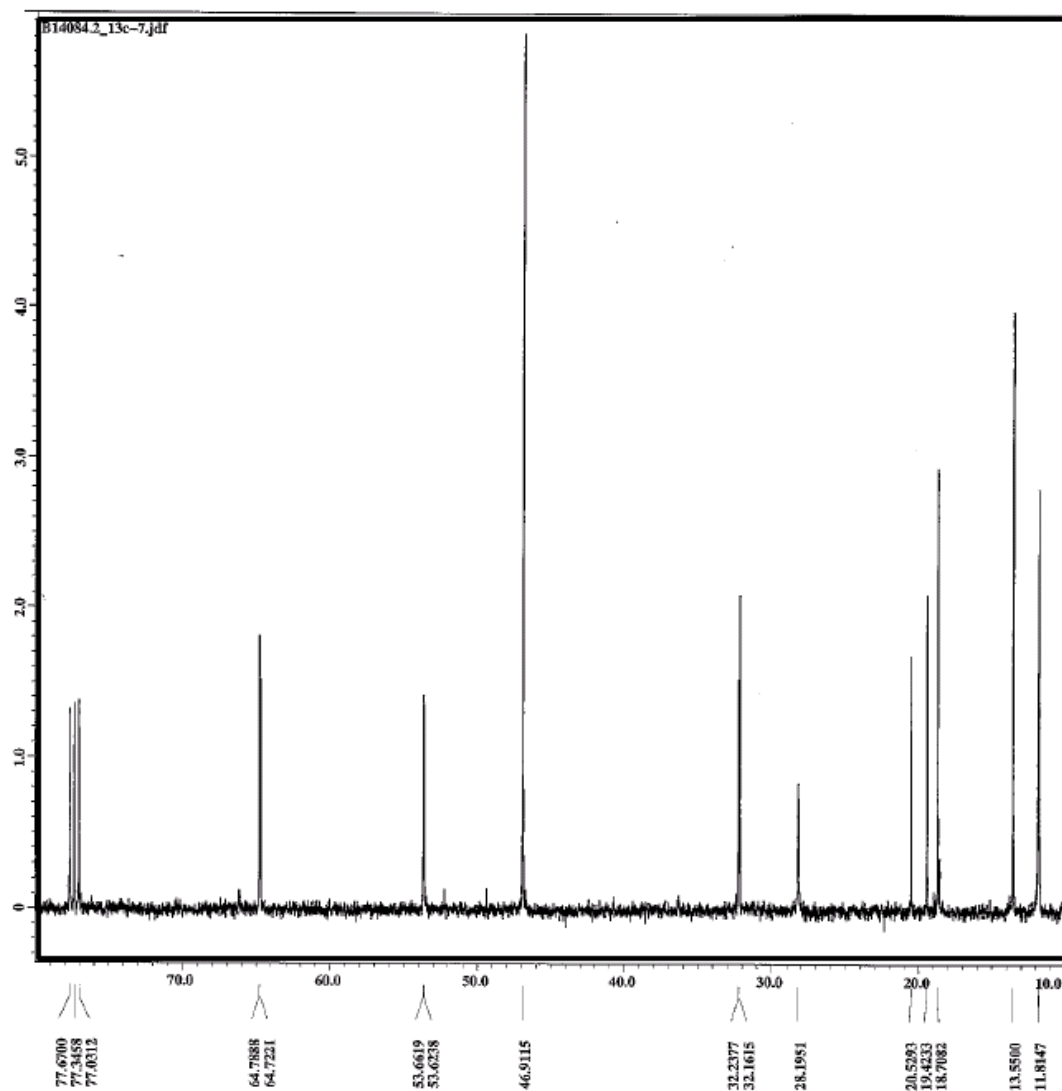


Figure 11.  $^{13}\text{C}$  NMR spectrum of EA 6043.

$^{31}\text{P}$  NMR ( $\text{CDCl}_3$ ,  $\delta$ ): 51.17. The small doublet (~4%) at 21.5 ppm in the  $^{31}\text{P}$  NMR is attributed to *O*-butyl methylpyrophosphate (VX pyro), a common synthesis impurity of EA 6043.

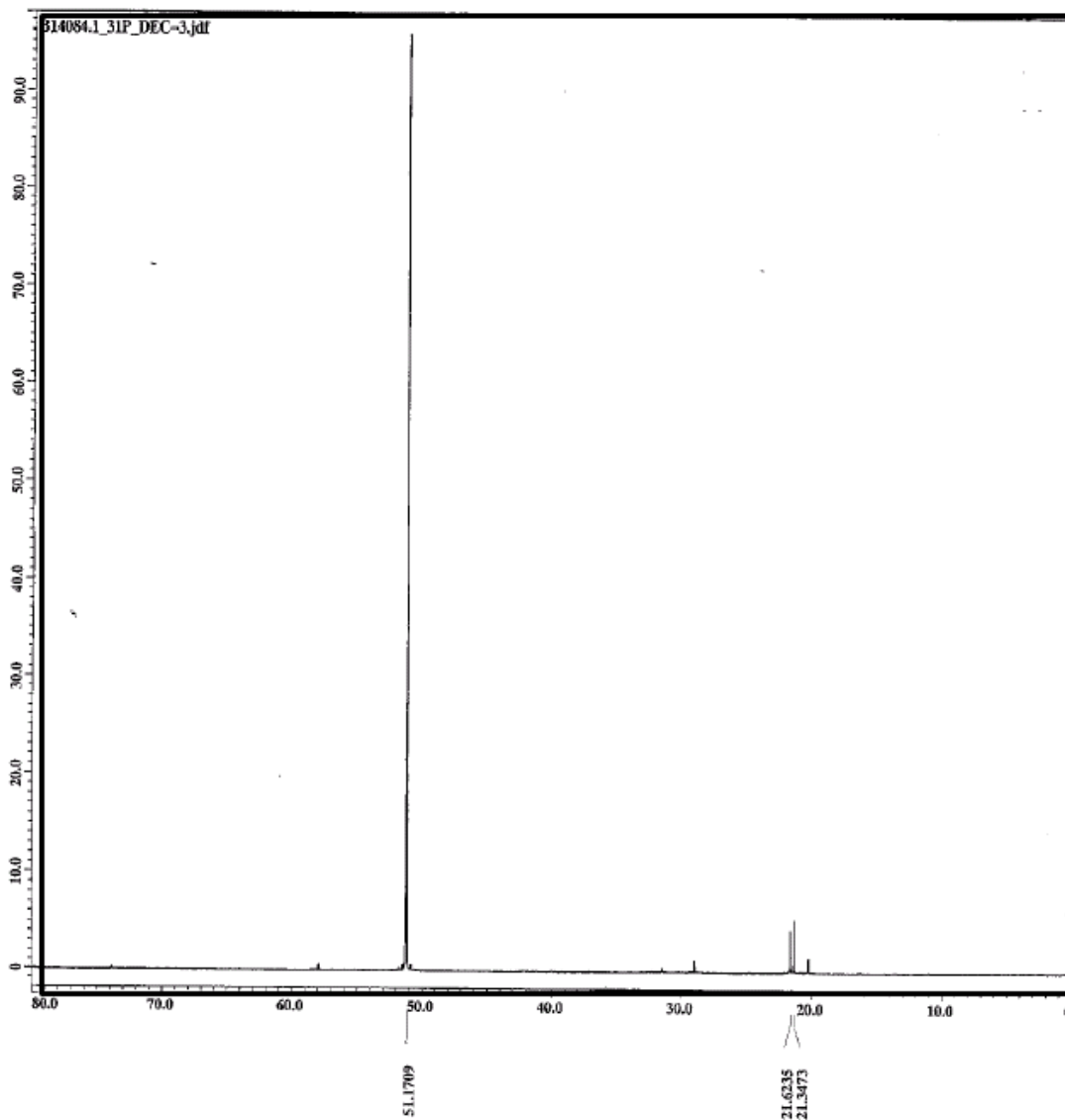


Figure 12.  $^{31}\text{P}$  NMR spectrum of EA 6043.

### 3.7 FTIR Spectroscopy

The FTIR spectrum of liquid-phase EA 6043 is shown in Figure 13.

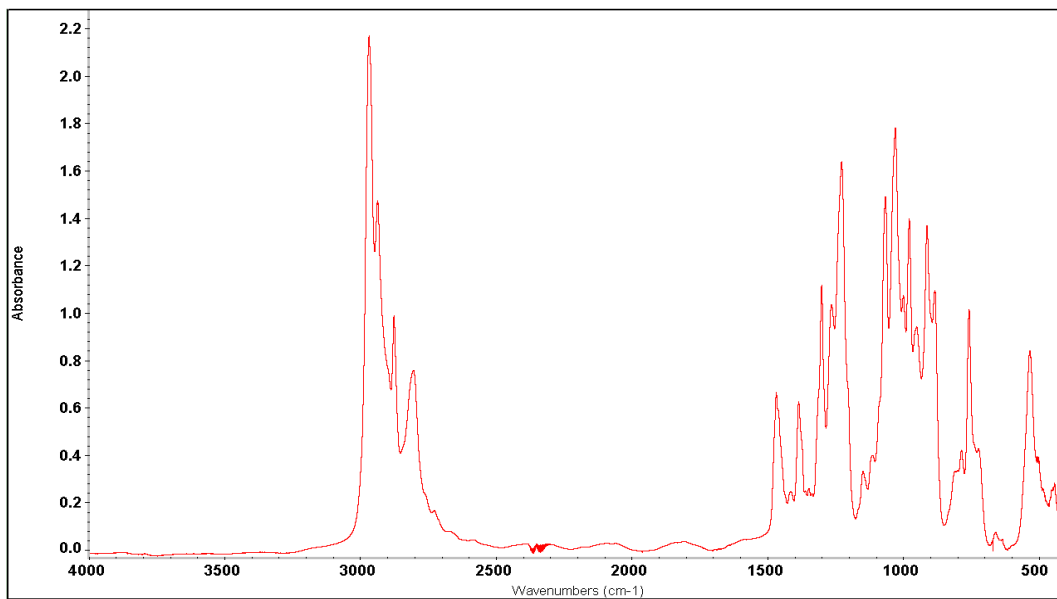


Figure 13. FTIR spectrum at 400–4000  $\text{cm}^{-1}$  for liquid-phase EA 6043.

The FTIR spectrum of vapor-phase EA 6043 is shown in Figure 14.

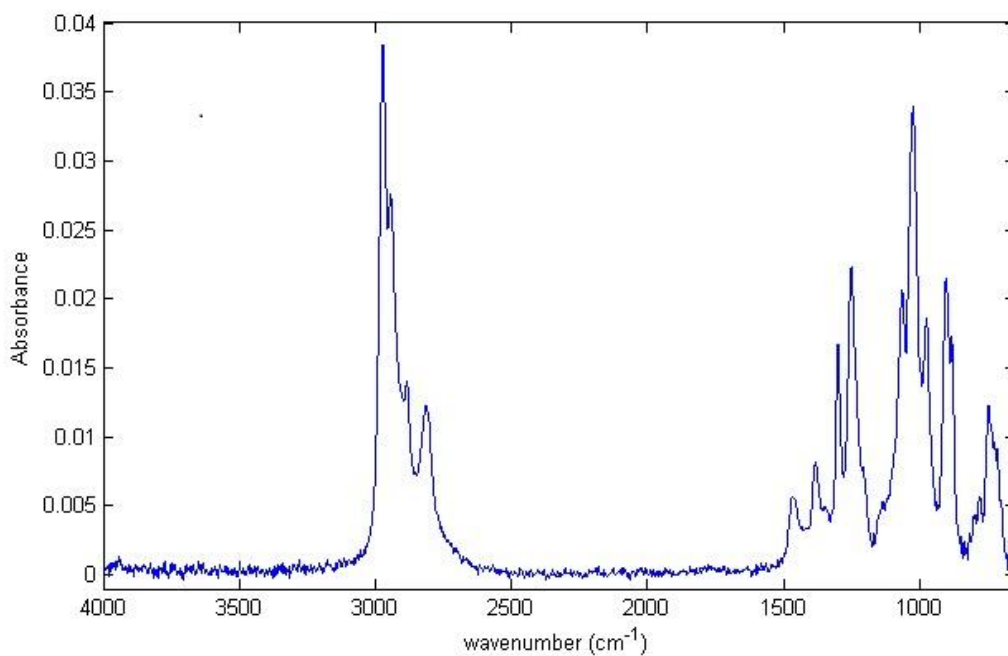


Figure 14. FTIR spectrum at 600–4000  $\text{cm}^{-1}$  for vapor-phase EA 6043.

### 3.8 Raman Spectroscopy

The Raman spectrum of liquid EA 6043 is shown in Figure 15.

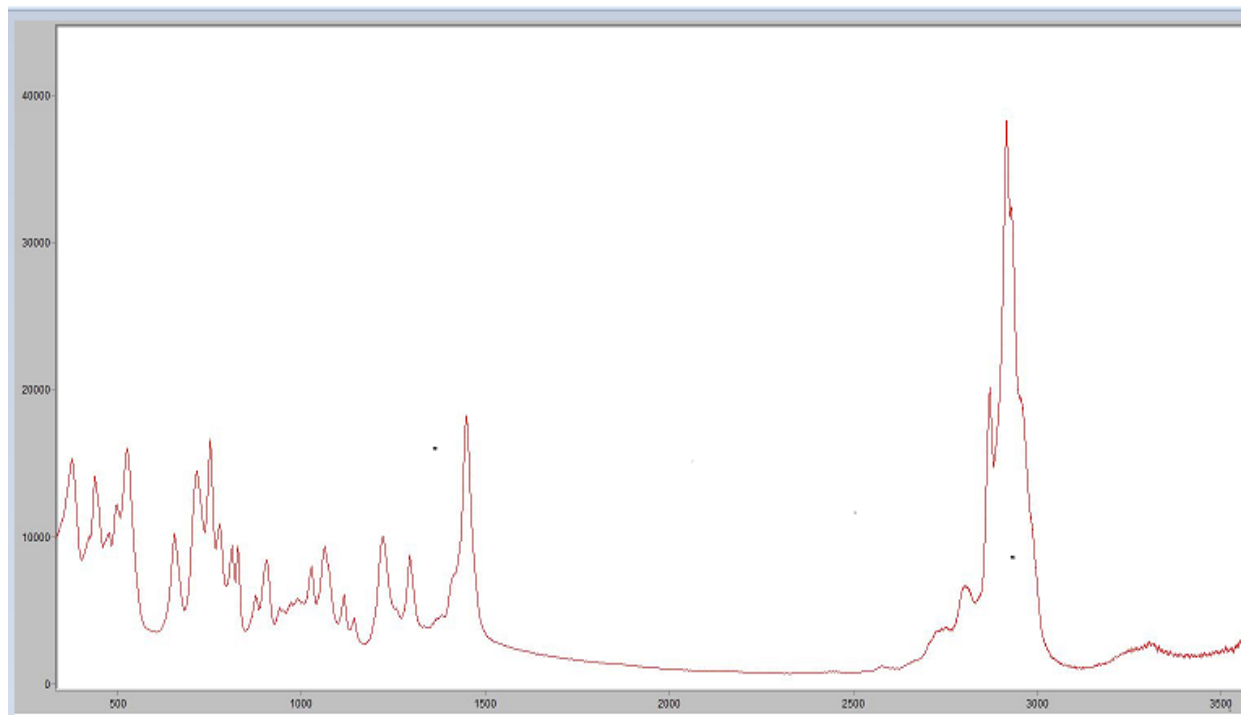


Figure 15. Raman spectrum of liquid-phase EA 6043 at  $\Delta\nu = 400\text{--}3600\text{ cm}^{-1}$ .

Table 9 provides a detailed listing of the FTIR absorptions for vapor- and liquid-phase and Raman-shift frequencies for EA 6043 that were observed in the current work.

Good agreement between vapor- and liquid-phase FTIR spectra is noted, although several small frequency shifts for the major absorptions were observed. These differences are also listed in Table 9.

Table 9. FTIR Absorption and Raman Shift Frequencies for EA 6043

FTIR Absorption (cm <sup>-1</sup> )		Difference (cm <sup>-1</sup> )	Raman Shift (cm <sup>-1</sup> )
Vapor	Liquid	Vapor - Liquid	Liquid
–	–	–	377
–	–	–	424
–	441	–	439
–	–	–	477
–	–	–	498
–	532	–	526
–	659	–	–
–	–	–	716
747	756	-9	753
–	–	–	–
–	784	–	777
–	–	–	811
–	–	–	828
882	882	0	877
905	911	-6	907
–	949	–	–
976	976	0	–
–	998	–	–
1025	1027	-2	1028
1064	1063	1	1064
–	1111	–	1116
–	1146	–	1144
1252	1225	27	1222
–	1262	–	–
1301	1299	2	1295
–	1346	–	–
1384	1383	1	–
–	1414	–	–
–	–	–	1449
1467	1466	1	–
2815	2802	13	–
–	2874	–	2870
~2915	–	–	2916
2944	2934	10	2930
2973	2966	7	–

#### 4. CONCLUSIONS

Selected physical properties, including density, viscosity, surface tension, and vapor pressure, were measured for EA 6043 and compared with those of its isomers, VX and RVX. These properties were measured at multiple temperatures when possible, and mathematical correlations have been determined to enable interpolation and limited extrapolation of the data. Several of the properties were measured using samples of varying purity yielding slightly different results.

The experimental density data for EA 6043 were fitted to a linear correlation with temperature. The density of EA 6043 is about 0.4% higher than that of VX and 0.6% higher than that of RVX.

Experimental viscosity data dependence on temperature for EA 6043 was correlated to a three-parameter Antoine equation. The viscosity of EA 6043 at 25 °C is 7% lower than VX and 3% higher than RVX.

Experimental surface tension data, reported at 20–35 °C for EA 6043, indicates that the surface tension of EA 6043 is lower than that of either VX or RVX.

Vapor pressure data for EA 6043 were measured using two complementary methods, and a three-parameter Antoine correlation has been derived to describe the data. The vapor pressure of EA 6043 is lower than that of VX and RVX throughout the temperature ranges investigated. Volatility and enthalpy and entropy of vaporization have been calculated based on the optimized Antoine constants.

All spectra, including mass spectrum,  $^1\text{H}$ ,  $^{13}\text{C}$ , and  $^{31}\text{P}$  NMR, FTIR, and Raman, reported herein, are consistent with the molecular structure of EA 6043.

Blank

## LITERATURE CITED

1. Buchanan, J.H.; Buettner, L.C.; Tevault, D.E. Vapor Pressure of Solid Bis(2-chloroethyl) Sulfide. *J. Chem. Eng. Data*, **2006**, *51*, 1331–1334.
2. Williams, B.R.; Butrow, A.B.; Samuels, A.C.; Miles, Jr., R.W.; Hulet, M.S. Vapor Pressure of Solid 1,4-Dithiane. *J. Chem. Eng. Data*, **2009**, *54*, 60–63.
3. Williams, B.R.; Hulet, M.S.; Brozena, A.; Miles, Jr., R.W.; Tevault, D.E. Vapor Pressure of 2-Dialkyl Aminoethanethiols. *J. Chem. Eng. Data*, **2013**, *58*, 1679–1684.
4. Brozena, A.; Tevault, D.E. Vapor Pressure of Thiodiglycol. *J. Chem. Eng. Data*, **2014**, *59* (2), 307–311.
5. Tevault, D.E.; Brozena, A.; Buchanan, J.H.; Abercrombie-Thomas, P.L. Thermophysical Properties of VX and RVX. *J. Chem. Eng. Data*, **2012**, *57* (7), 1970–1977.
6. Buchanan, J.H.; Buettner, L.C.; Butrow, A.B.; Tevault, D.E. *Vapor Pressure of VX*; ECBC-TR-068; U.S. Army Edgewood Chemical Biological Center: Aberdeen Proving Ground, MD, 1999; UNCLASSIFIED Report (ADA371297).
7. Buchanan, J.H.; Butrow, A.B.; Abercrombie, P.A.; Buettner, L.C.; Tevault, D.E. *Vapor Pressure of Russian VX*; ECBC-TR-480; U.S. Army Edgewood Chemical Biological Center: Aberdeen Proving Ground, MD, 2006; UNCLASSIFIED Report (ADA447993).
8. Butrow, A.B.; Buchanan, J.H.; Tevault, D.E. Vapor Pressure of Organophosphorus Nerve Agent Simulant Compounds. *J. Chem. Eng. Data*, **2009**, *54* (6), 1876–1883.
9. ASTM D 4052, *Standard Test Method for Density, Relative Density, and API Gravity of Liquids by Digital Density Meter*; ASTM International: West Conshohocken, PA, 2011.
10. ASTM D 445, *Standard Test Method for Kinematic Viscosity of Transparent and Opaque Liquids (the Calculation of Dynamic Viscosity)*; ASTM International: West Conshohocken, PA, 2001.
11. Abercrombie-Thomas, P.L.; Butrow, A.B.; Buchanan, J.H. *Selected Physical Properties of 2-Chloroethyl-3-Chloropropyl Sulfide (CECPRS)*; ECBC-TR-804; U.S. Army Edgewood Chemical Biological Center: Aberdeen Proving Ground, MD, 2010; UNCLASSIFIED Report (ADA531948).
12. Davies, J.T.; Rideal, E.K. *Interfacial Phenomena*; Academic Press: New York, 1963; p. 46.
13. ASTM E 1782, *Standard Test Method for Determining Vapor Pressure by Thermal Analysis*; ASTM International: West Conshohocken, PA, 2014.
14. ASTM E 967, *Standard Test Method for Temperature Calibration of Differential Scanning Calorimeters and Differential Thermal Analyzers*; ASTM International: West Conshohocken, PA, 2014.

15. ASTM E 1194, *Standard Test Method for Vapor Pressure*; ASTM International: West Conshohocken, PA, 2001.
16. IUPAC. *Recommended Reference Materials for the Realization of Physicochemical Properties*; Marsh, K.N., Ed.; Blackwell Scientific Publications: Oxford, U.K., 1987.
17. Cox, R.A.; McCartney, M.J.; Culkin, F. The Specific Gravity/Salinity/Temperature Relationship in Natural Seawater. *Deep-Sea Res.* **1970**, *17* (4), 679–689.
18. Thomson, G.W. The Antoine Equation for Vapor-Pressure Data. *Chem. Rev.* **1946**, *38* (1), 1–39.
19. Brozena, A. Vapor Pressure of 1-Octanol below 5 kPa Using DSC. *Thermochim. Acta* **2013**, *561*, 72–76.

## ACRONYMS AND ABBREVIATIONS

$^1\text{H}$ NMR	proton nuclear magnetic resonance
$^{13}\text{C}$ NMR	carbon-13 nuclear magnetic resonance
$^{31}\text{P}$ NMR	phosphorus-31 nuclear magnetic resonance
CCD	charge-coupled device
DSC	differential scanning calorimetry
EA 6043	<i>O</i> -( <i>n</i> -butyl)- <i>S</i> -(2-diethylaminoethyl) methylphosphonothiolate
EI-MS	electron impact-mass spectrometry
FTIR	Fourier transform infrared
FPD	flame photometric detector
FPD-P	flame photometric detector with a phosphorus filter
GC	gas chromatography
MCT	mercury-cadmium telluride
<i>m/z</i>	mass-to-charge ratio
NIR	near infrared
NIST	National Institute of Standards and Technology
NMR	nuclear magnetic resonance
$P_{\text{exp}}$	experimental vapor pressure
$P_{\text{calc}}$	calculated vapor pressure
RVX	Russian VX, <i>O</i> -isobutyl- <i>S</i> -(2-diethylaminoethyl) methylphosphonothiolate
TGS	triglycine sulfate
VX	<i>O</i> -ethyl- <i>S</i> -(2-diisopropylaminoethyl) methylphosphonothiolate
VX pyro	<i>O</i> -butyl methylpyrophosphate





